

AtALMT1, which encodes a malate transporter, is identified as one of several genes critical for aluminum tolerance in *Arabidopsis*

Owen A. Hoekenga^{*†}, Lyza G. Maron^{**}, Miguel A. Piñeros^{**}, Geraldo M. A. Cançado^{*§}, Jon Shaff^{**}, Yuriko Kobayashi[¶], Peter R. Ryan^{||}, Bei Dong^{||}, Emmanuel Delhaize^{||}, Takayuki Sasaki^{**}, Hideaki Matsumoto^{**}, Yoko Yamamoto^{**}, Hiroyuki Koyama[¶], and Leon V. Kochian^{†,††}

^{*}Boyce Thompson Institute for Plant Research, Ithaca, NY 14853; [†]U.S. Plant, Soil, and Nutrition Laboratory, U.S. Department of Agriculture–Agricultural Research Service, and [‡]Department of Plant Biology, Cornell University, Ithaca, NY 14853; [§]Center for Molecular Biology and Genetic Engineering, State University of Campinas, 13083-970, Campinas, Sao Paulo, Brazil; [¶]Faculty of Applied Biological Sciences, Gifu University, Gifu 501-1193, Japan; ^{||}Division of Plant Industry, Commonwealth Scientific and Industrial Research Organization, Canberra ACT 2601, Australia; and ^{**}Research Institute for Bioresources, Okayama University, Kurashiki 710-0046, Japan

Communicated by Deborah P. Delmer, The Rockefeller Foundation, New York, NY, April 7, 2006 (received for review November 21, 2005)

Aluminum (Al) tolerance in *Arabidopsis* is a genetically complex trait, yet it is mediated by a single physiological mechanism based on Al-activated root malate efflux. We investigated a possible molecular determinant for Al tolerance involving a homolog of the wheat Al-activated malate transporter, *ALMT1*. This gene, named *AtALMT1* (At1g08430), was the best candidate from the 14-member *AtALMT* family to be involved with Al tolerance based on expression patterns and genomic location. Physiological analysis of a transferred DNA knockout mutant for *AtALMT1* as well as electrophysiological examination of the protein expressed in *Xenopus* oocytes showed that *AtALMT1* is critical for *Arabidopsis* Al tolerance and encodes the Al-activated root malate efflux transporter associated with tolerance. However, gene expression and sequence analysis of *AtALMT1* alleles from tolerant Columbia (Col), sensitive Landsberg *erecta* (Ler), and other ecotypes that varied in Al tolerance suggested that variation observed at *AtALMT1* is not correlated with the differences observed in Al tolerance among these ecotypes. Genetic complementation experiments indicated that the Ler allele of *AtALMT1* is equally effective as the Col allele in conferring Al tolerance and Al-activated malate release. Finally, fine-scale mapping of a quantitative trait locus (QTL) for Al tolerance on chromosome 1 indicated that *AtALMT1* is located proximal to this QTL. These results indicate that *AtALMT1* is an essential factor for Al tolerance in *Arabidopsis* but does not represent the major Al tolerance QTL also found on chromosome 1.

abiotic stress | electrophysiology | genetics | organic acid exudation

Low pH is a major soil constraint to agricultural production, reducing yield on nearly 25% of the world's land presently under production (1). At pH < 5.5, the rhizotoxic Al³⁺ cation is solubilized into soil solution from aluminosilicate clay complexes to levels that inhibit root growth and function (2). The stunted, poorly functioning root systems that result from aluminum (Al) toxicity directly translate into reduced plant vigor and yield, increasing susceptibility to other stressors such as drought, nutrient deficiency, and herbivory. Al toxicity is the primary limitation on crop production for 38% of farmland in Southeast Asia, 31% of farmland in Latin America, and ≈20% of farmland in East Asia, sub-Saharan Africa, and North America (1). Thus, Al toxicity reduces food security in many parts of the world where it is most tenuous. In addition, in developed countries, high-input farming practices, including the excessive use of ammonia fertilizers, acidify previously neutral soils (3). Although chemical amendments such as lime can neutralize soil acidity, this option is not economically feasible for poor farmers, nor is it an effective strategy for alleviating subsoil acidity (4).

The best documented physiological mechanism for plant Al tolerance involves the Al-activated release of organic acids from

roots (summarized in ref. 5). These organic acids are deprotonated anions at the pH found in the cytosol; once transported out of the root, they can effectively chelate Al³⁺ in the rhizosphere to form complexes that are not rhizotoxic (2, 5). For example, Al-activated root malate release has been reported as an Al tolerance mechanism for *Arabidopsis* and wheat, and citrate release has been reported for maize Al tolerance (6–8). The rate of organic acid anion exudation is highly correlated with the overall degree of Al tolerance in *Arabidopsis* and wheat, suggesting that the majority of differences in Al tolerance between varieties within these species can be explained by this single physiological mechanism (6, 9). However, in other species such as maize, it is clear that Al tolerance has a more complex genetic and physiological basis, where organic acid release plays a significant but not exclusive role in determining overall Al tolerance (10).

Al-activated malate release from wheat roots is mediated by *ALMT1* (*Al-activated malate transporter 1*), the first Al tolerance gene cloned from any plant (11). The gene is constitutively expressed in wheat root apices (11, 12), whereas the *ALMT1* protein is localized to the plasma membrane. These features are consistent with its role as a malate efflux transporter in roots (13). The *ALMT1* locus is linked to variation in Al tolerance levels in several wheat mapping populations, and the level of *ALMT1* gene expression was correlated with overall Al tolerance across 13 wheat cultivars ($r^2 = 0.86$) (12). Raman *et al.* (12) concluded that *ALMT1* is the major Al tolerance locus in wheat.

Arabidopsis uses root malate release as its primary Al tolerance mechanism (6), but, unlike wheat, the inheritance of Al tolerance in *Arabidopsis* is complex. In a previous study from our lab, two quantitative trait loci (QTLs) were detected that explained 40% of the variance in Al tolerance and malate release (6). An *in silico* analysis of the *Arabidopsis* genome indicated that it contains a number of sequences similar to *ALMT1* (11). These observations led us to ask the following questions: Given the similarity between *Arabidopsis* and wheat with respect to the physiology of Al tolerance, are there one or more *ALMT1*-like genes relevant to Al tolerance responses in *Arabidopsis*? If so, how do they fit into the existing model for Al tolerance for *Arabidopsis*?

Conflict of interest statement: No conflicts declared.

Abbreviations: Col, Columbia; Ler, Landsberg *erecta*; MT, mutant; QTL, quantitative trait locus.

Data deposition: The sequences reported in this paper have been deposited in the GenBank database (accession nos. DQ465038–DQ465042).

^{††}To whom correspondence should be addressed. E-mail: lvk1@cornell.edu.

© 2006 by The National Academy of Sciences of the USA



Fig. 1. Locations of *ALMT1*-like genes in *Arabidopsis thaliana*. *ALMT* defines a family of genes in *Arabidopsis*, whose members are listed by gene number (e.g., on chromosome 1, "08430" corresponds to At1g08430). These *AtALMT* family members also are numbered based on their location in the *Arabidopsis* genome. Gene numbers in black denote genes with evidence for expression in roots (14). Genes outlined with boxes exhibit tissue-specific expression patterns within the root (15).

Results

Using wheat *ALMT1* as a query, multiple similar genes can be identified in *Arabidopsis* by using TBLASTX at the National Center for Biotechnology Information. We propose naming these genes the *AtALMT* family and assigning numbers based on their position in the genome (Fig. 1). The most similar predicted *Arabidopsis* protein to wheat *ALMT1* is *AtALMT8* (At3g11680), which is 44% identical and 64% similar to wheat *ALMT1* over its 399-aa length.

Several genome-wide estimates for gene expression exist for *Arabidopsis*. One is the massively parallel signature sequencing data set; *ALMT1*-like genes with evidence for expression in roots (ROF, ROS, or GSE libraries) are noted in black on Fig. 1 (14). In addition, Birnbaum *et al.* (15) produced a gene expression atlas for the *Arabidopsis* root, reporting only those genes that demonstrated differences in expression due to tissue localization or developmental stage. Only two of the *ALMT1*-like genes have specific patterns of expression within the root; *AtALMT1* is most highly expressed in epidermal cells of the root, and *AtALMT12* is expressed in the endodermis (15). Thus, of the 14 members of the *ALMT1*-like gene family in *Arabidopsis*, *AtALMT1* presents itself as the best candidate Al tolerance gene because it is expressed in the tissue most likely to be associated with root malate release into the rhizosphere.

We examined *AtALMT1* expression in nine ecotypes with varying Al tolerance to verify whether gene expression was consistent with a possible role in Al tolerance. *AtALMT1* is expressed in roots and induced by Al treatment (Fig. 2) but is not expressed in shoots (data not shown). Al tolerance levels for the ecotypes used for the gene expression study were determined by root growth and malate release assays (Fig. 8, which is published as supporting information on the PNAS web site). These varieties can be grouped in five distinct tolerance classes based on root growth in the presence of Al, in descending order of

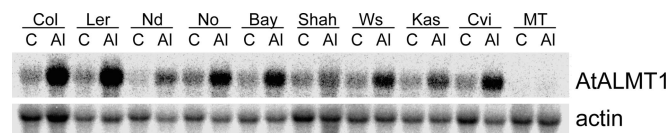


Fig. 2. *AtALMT1* is Al-inducible. (Upper) Northern blot analysis was used to test expression of *AtALMT1* in control and Al-stressed roots. (Lower) The blot was rehybridized with an actin probe to demonstrate equivalent loading. Nine ecotypes that vary widely in tolerance were used for this experiment, plus the *AtALMT1* MT in the Col background.

Table 1. Amino acid polymorphisms between *AtALMT1* alleles from six *Arabidopsis* ecotypes varying in Al tolerance (high to low)

Residue no.	Cape Verde					
	Niederzenz	Col	Islands	Nossen	Bayreuth	Ler
33	G	V	V	V	V	V
36	A	S	S	A	A	A
194	S	S	S	S	F	S
375	V	V	I	V	V	V

tolerance: Niederzenz and Kashmir; Columbia (Col) and Shakdara; Cape Verde Islands, Nossen, and Wassilewskija; and Bayreuth and Landsberg *erecta* (Ler); and a homozygous transferred DNA insertion mutant (MT) (SALK no. 009629), for *AtALMT1* (16). *AtALMT1* is not expressed in the MT, where the gene is disrupted in the first exon. *AtALMT1* was cloned and sequenced from six of the nine ecotypes shown in Fig. 2; *AtALMT1* is less polymorphic ($\Theta = 0.0032$) compared with the average *Arabidopsis* gene ($\Theta = 0.007$; refs. 17 and 18). Four SNPs were detected in *AtALMT1* that alter protein sequence such that one or two amino acid residues differed among the predicted proteins relative to Col (Table 1). However, no correlations between either the polymorphisms observed in the different *AtALMT1* alleles or levels of gene expression were found with Al tolerance for the ecotypes studied.

The *AtALMT1* MT grew as well as WT Col in soil, low-pH hydroponic culture, and on agar plates. Fig. 3A shows WT and MT Col grown on low-pH solid medium. However, when Al^{3+} was introduced into medium, the MT was much more Al sensitive, with significantly shorter roots than WT ($P < 0.001$; Fig. 3B). This result is observed in both solid and liquid culture environments (Fig. 8). The decrease in tolerance in the MT was correlated with a near complete loss of Al-activated root malate efflux (Fig. 4). In the absence of Al stress, the roots of MT and WT Col plants released similar low amounts of malate and citrate after 2 d in hydroponic culture. In the presence of Al stress, root malate release significantly increased in WT Col, whereas citrate release was inhibited. In contrast, the *AtALMT1* MT lacked any Al-activated malate release.

Heterologous expression of *AtALMT1* in *Xenopus laevis* oocytes supports its characterization as an Al-activated malate efflux transporter. The two-electrode voltage clamp method measured the net currents in oocytes expressing *AtALMT1* both in the

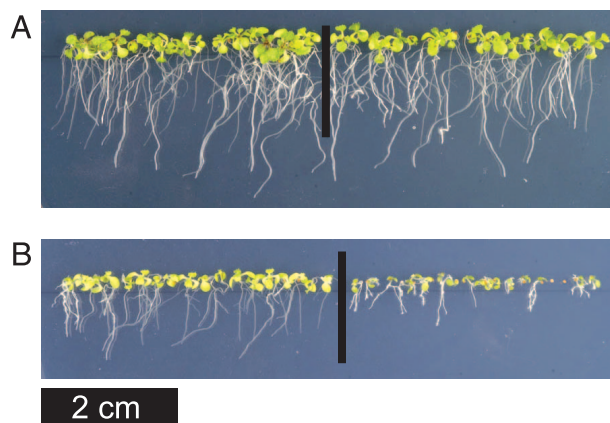


Fig. 3. *AtALMT1* MT is Al-sensitive. (A) WT Col (Left) and MT Col (*AtALMT1* knockout) (Right) grown on solid medium (no Al and pH 4.20). (B) WT Col (Left) and MT Col (Right) grown on solid medium imbued with 500 μ M $AlCl_3$ (pH 4.20).

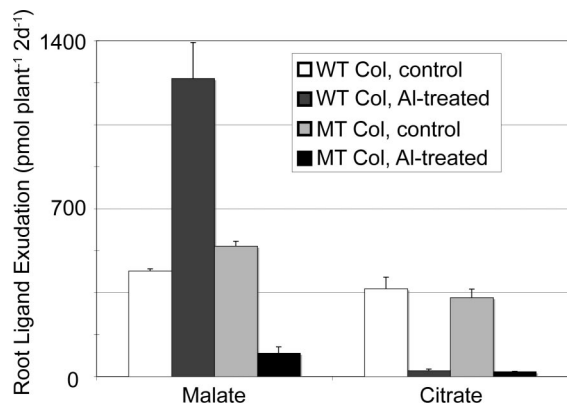


Fig. 4. Al-activated root organic acid exudation in hydroponic culture. Al-activated root exudation of malate and citrate was profiled in the root exudate solutions from WT and *AtALMT1* MT plants grown in hydroponic culture. Dark gray histograms denote +Al-treated roots; light gray denotes control-treated plants. Median values are shown; error bars reflect standard error.

absence and presence of Al. As seen in Fig. 5A, the presence of Al in the bathing solution activated a negative current (consistent with malate efflux) in cells preloaded with malate and expressing *AtALMT1*. In contrast, control cells preloaded with malate did not show any inward currents activated by Al. Representative current traces recorded under voltage-clamp conditions for a range of voltages are depicted in Fig. 9, which is published as supporting information on the PNAS web site. The current-to-voltage relationships derived from these traces are shown in Fig. 5B and C. Cells expressing *AtALMT1* not exposed to Al had a significantly larger inward current than did control cells, whether they had or had not been preloaded with malate, although the current was greater in malate-loaded cells. For both unloaded and malate-loaded cells expressing *AtALMT1*, addition of Al to the bathing media resulted in a 2-fold increase in the magnitude of the *AtALMT1*-mediated inward current. This enhancement was reversible upon removing Al from the bathing media. This result indicates that although Al

enhances the activity of *AtALMT1*, this protein has intrinsic properties that allow it to function as a malate efflux transporter in the absence of Al (at least in oocytes).

The identity of the inward current mediated by *AtALMT1* was also inferred from the current-to-voltage relationships (Fig. 5B and C). The increase in current magnitude due to Al in malate-preloaded cells was significant at holding potentials more negative than -50 mV. In contrast, when the cells were not preloaded with malate, these differences were only evident at holding potentials more negative than -160 mV. In addition, the increase in the intracellular malate concentration (an ≈ 1.3 mM increase in intracellular malate, assuming a 1-mm oocyte diameter) in *AtALMT1*-expressing cells resulted in a positive 25-mV shift (from -30 to ± 5 mV) in the reversal potential (i.e., the voltage at which the net current is 0). This shift in reversal potential of the inward current is consistent with *AtALMT1* currents being mediated by anion efflux. In contrast, control cells showed no significant shift in the reversal potential under the same conditions. The increase in current magnitude and the shift in the reversal potential upon increasing the intracellular malate concentration indicate that *AtALMT1* is capable of mediating an Al-enhanced malate efflux from the cell.

QTL analyses had previously detected major Al tolerance loci in the vicinity of *AtALMT1* (6, 19). None of the polymorphisms detected in 3 kb of DNA sequence at *AtALMT1* were correlated with differential Al tolerance (Table 1); however, it is possible that polymorphisms at *AtALMT1* are responsible for the differences in Al tolerance between Ler and Col. A genetic complementation experiment was used to test this possibility, crossing the Al-sensitive Ler as a pollen donor onto the *AtALMT1* MT (Col background). If the Ler allele is inferior to Col, then the F_1 should be more Al sensitive than WT Col. If the alleles are equivalent, then the F_1 should be similar in Al tolerance to WT Col. Ecotype Col plants, both WT and MT, were grown alongside WT Ler and the F_1 seedlings. As shown in Fig. 6, the F_1 plants exhibited a similar level of Al tolerance and Al-activated malate release as the WT Col; these responses in the F_1 were significantly greater ($P < 0.05$) than those seen in either the *AtALMT1* MT or in WT Ler parents. These findings strongly suggest that variation at *AtALMT1* is insignificant and thus not does represent a major Al tolerance QTL.

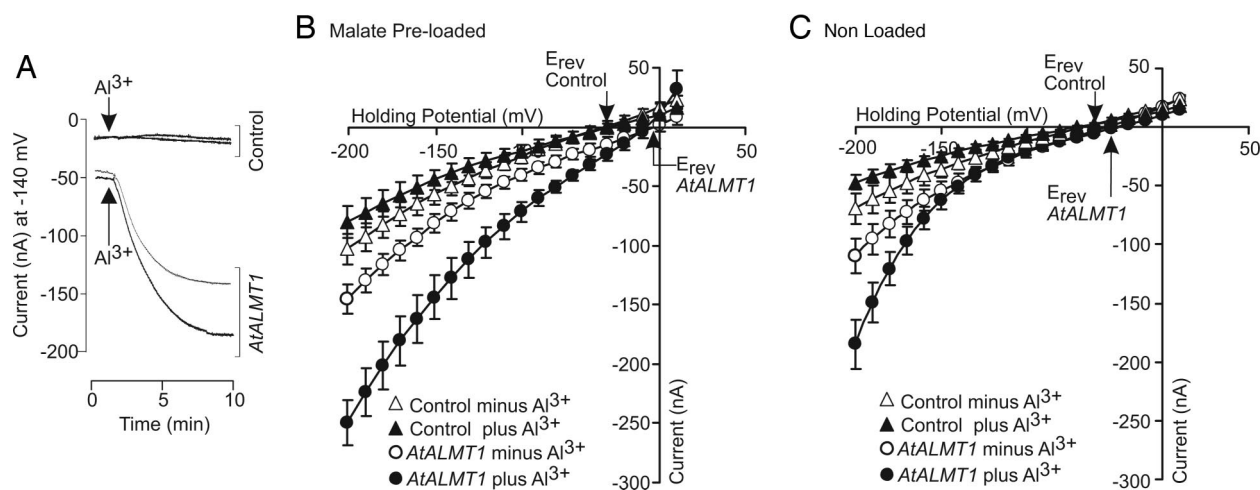


Fig. 5. Electrophysiological characterization of *AtALMT1* expressed in *X. laevis* oocytes. (A) Al^{3+} -induced activation of an inward current in oocytes expressing *AtALMT1* and preloaded with malate. Net currents were recorded at -140 mV. The arrow indicates the time point when the bathing solution was exchanged with a solution containing Al^{3+} . Each trace was recorded from a different cell. (B and C) Mean current-to-voltage relationships from control (triangles) and *AtALMT1*-expressing (circles) oocytes recorded in the absence (open symbols) or presence (filled symbols) of Al^{3+} . B and C show the relationship obtained for cells preloaded or not loaded with malate, respectively. Each value represents the average of at least 10 different cells; error bars denote standard error. E_{rev} represents the reversal potential (i.e., the voltage at which the net current is 0) and is indicated by the arrows. The data shown represent the average of currents recorded in batches of oocytes from three different donor frogs.

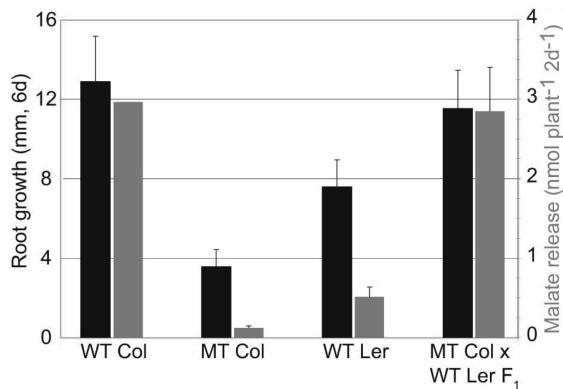


Fig. 6. Genetic complementation of transferred DNA-induced mutation at *AtALMT1*. Root growth (black bars) and root malate release (gray bars) in the presence of Al^{3+} were profiled in WT Col, WT Ler, MT Col, and F_1 seedlings from a cross of WT Ler and the *AtALMT1* MT Col. Median values are shown; error bars indicate standard error.

In parallel to reverse genetics, we also used forward genetics to characterize the Al tolerance gene detected on chromosome 1. Molecular markers were designed to flank the confidence interval for the primary QTL on chromosome 1 and used to screen F_2 individuals from a cross between Ler and Col to identify recombinants (Table 2, which is published as supporting information on the PNAS web site). Fig. 7 shows the result of an experiment wherein 41 F_3 families were grown in a duplicated, randomized block design. A correlation analysis was performed to associate allelic state at each of the markers with family median root growth after 6 d in Al by using an empirical significance threshold. These experiments reconfirmed the initial QTL analysis, because a significant Al tolerance locus was detected in the vicinity of 1 megabase (Mb) on chromosome 1 by using an independent population derived from the same Col and Ler ecotypes [position 1–5 cM on the Lister and Dean genetic map (20)]. What appeared as a broad peak in the previous composite interval mapping analysis of recombinant inbred lines separates into two distinct peaks in the $F_{2,3}$ population. A third peak is obvious in this analysis near 2.7 Mb but did not exceed the significance threshold. This peak is highlighted because *AtALMT1* is located near this third peak (marked with an asterisk in Fig. 7). Thus, the physical and genetic

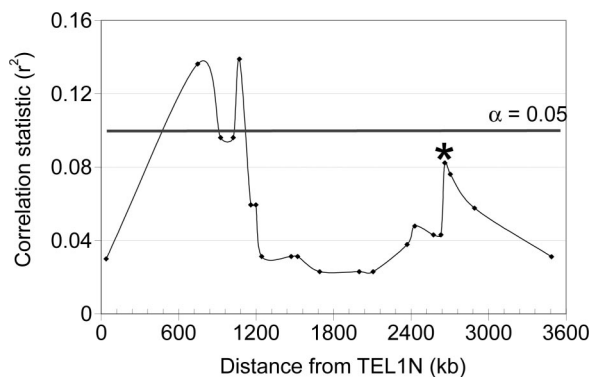


Fig. 7. Fine-scale mapping of Al tolerance QTL on chromosome 1. Forty-one $F_{2,3}$ families were genotyped at 23 genetic markers from the distal end of chromosome 1N. These families were subsequently phenotyped for root length after 6 d of growth in nutrient solution with an Al^{3+} activity at 1.5 μM . A correlation analysis was performed by using an empirically determined significance threshold ($\alpha = 0.05$, gray line) and is plotted here.

location for *AtALMT1* is not consistent with the location for the principal Al tolerance locus (or loci) on chromosome 1.

Discussion

Hoekenga *et al.* (6) identified Al-activated root malate release as the primary Al tolerance mechanism in *Arabidopsis* and showed that Al tolerance genes detected by QTL analysis in the Ler \times Col recombinant inbred population regulate this tolerance process. In the current study, physiological analysis of the *AtALMT1* MT confirmed the importance of the *AtALMT1* gene to *Arabidopsis* Al tolerance; the MT exhibited a dramatic inhibition of root growth in the presence of Al and lacked Al-activated malate release (Figs. 3 and 4). Thus, the *AtALMT1* protein is responsible for the Al-activated root malate release. It is not responsible for the moderate level of malate (and citrate) release seen in the absence of Al, because under control conditions, the MT exhibits a level of malate efflux comparable to that of WT. This pattern indicates that two root malate transporters are responsive to Al, because Al activates *AtALMT1* while inhibiting a second unidentified transporter. None of the other *AtALMT* proteins expressed in the root (Fig. 1) are redundant in function to *AtALMT1* with regard to Al tolerance, because once *AtALMT1* is absent, no root malate release is observed in the presence of Al. Malate release is also correlated with Al tolerance in the nine ecotypes tested ($r = 0.71$; Fig. 8), suggesting that malate release is a broadly important Al tolerance mechanism in *Arabidopsis*. However, because nearly 30% of the variation in tolerance did not correlate with malate release, it appears that in the most tolerant ecotypes, one or more additional tolerance mechanisms may be operating in conjunction with malate release.

Al regulates both the expression of the *AtALMT1* gene (Fig. 2) and the transport activity of the protein (Figs. 4 and 5), unlike in wheat, where *ALMT1* is constitutively expressed (11). The biophysical properties of oocytes expressing *AtALMT1* demonstrate that Al enhances anion transport mediated by *AtALMT1* (Fig. 5A), whereas shifts in the reversal potential indicate that the protein mediates malate efflux (Fig. 5B and C). Therefore, at least one homologous gene in both wheat and *Arabidopsis* is important for Al tolerance; *AtALMT1* mediates malate release in response to Al stress and is the essential final step in this Al tolerance pathway.

AtALMT1 is easily placed into our existing model for Al tolerance. First, the biophysical analysis of *AtALMT1* expressed in *Xenopus* oocytes indicates that the basal state of the protein is that of an ion channel mediating anion efflux (Fig. 5B). This activity increases with the presence of Al, but the transporter has the capacity to efflux anions from *Xenopus* oocytes without Al activation. Second, genetic complementation tested the efficacy and activity of the Ler allele of *AtALMT1*. If polymorphisms at *AtALMT1* were detected by QTL analysis, then the Ler allele should be markedly less effective than the Col allele. The F_1 s, which are hemizygous at *AtALMT1* and heterozygous everywhere else, grew very much like WT Col in Al and were far more Al tolerant than either WT Ler or MT Col (Fig. 6). Furthermore, the F_1 plants exhibited rates of Al-activated malate exudation comparable to that observed in WT Col. This finding indicates that a single copy of *AtALMT1-Ler* is capable of mediating malate transport as well as two copies of the Col allele, in contrast to the result obtained from WT Ler plants, where the same protein in the Ler genetic environment transports a significantly smaller amount of malate. This result suggests that factors exist to regulate *AtALMT1*-mediated malate release, so that the Ler allele can be activated by Col native factors and mediate a Col-type malate release in a hybrid. Third, fine-scale genetic mapping indicates that the major Al tolerance genes associated with the QTL on chromosome 1 occur within the 500- to 1,200-kb interval, which is distal to *AtALMT1* (Fig. 7). Taken together, these results indicate that although *AtALMT1* is the

essential final factor for Al tolerance in *Arabidopsis*, it is not the Al tolerance gene previously detected by QTL analysis on chromosome 1.

The location of the Al tolerance QTL discussed here is different from that identified by Kobayashi and Koyama (19). In that study, a higher pH (5.0) was used with a nutrient solution with lower ionic strength and likely different Al speciation. Their primary QTL was found within an interval that is inconsistent with both our prior and present results, indicating that different genetic factors are important for responses to these two different environments. However, the *AtALMT1* MT is also Al sensitive in the pH-5.0 medium (Y.K. and H.K., unpublished data), indicating that the malate transporter is required for Al tolerance responses in both environments. How these two environments differ while eliciting convergent physiological responses is currently unknown.

It is intriguing that we have identified one or more Al tolerance loci physically located on chromosome 1 near the *AtALMT1* gene encoding the transporter facilitating malate efflux. Could one or more Col native *AtALMT1* activating factors be responsible for the tolerance QTL on chromosome 1, and, if so, what are they? Al-activated malate release can be dissected into three components: perception of exogenous Al and transduction of this signal into the cell, production of malate, and transport of malate out of the root. Characterization of *AtALMT1* places this protein at the final step of this tolerance process, whereas some of these other factors may have been detected by means of the genetic analyses. When we examine the chromosomal interval spanned by the two QTL peaks shown in Fig. 7, there are a number of candidates for an *AtALMT1* activator, including possible signal perception and transduction proteins, as well as several with potential protein–protein interaction domains. In contrast, malate synthesis-related genes are essentially absent from this region, which leads us to emphasize the importance of proteins that may help regulate *AtALMT1* as candidate Al tolerance genes. These genes will need to be evaluated in the search for the gene or genes responsible for the Al tolerance QTL and their possible direct interaction with *AtALMT1*. Given the utility of wheat *ALMT1* for crop improvement purposes using transgenic barley (21), developing a deeper understanding of the regulation of ALMT1-related proteins should provide additional opportunities for increasing Al tolerance in economically important plant species.

Materials and Methods

Plant Growth Conditions and Analytical Methodologies. *Arabidopsis* seedlings were grown on solid media and in liquid culture as described in ref. 6 with the following modifications. For liquid culture, the initial (high strength) nutrient solution was composed of 3 mM MgCl₂, 0.25 mM (NH₄)₂SO₄, 1 mM Ca(NO₃)₂, 2 mM KCl, 2.75 mM CaCl₂, 2 mM Homopipes (pH 4.20, adjusted with 10 M KOH), 1% (wt/vol) sucrose, 0.18 mM KH₂PO₄, 0.0136 mM AlCl₃, and micronutrients as previously described. Magenta tissue culture vessels were assembled with polycarbonate stands and polypropylene mesh as previously described but autoclaved empty and dry. The nutrient solution was prepared by omitting both KH₂PO₄ and AlCl₃ and then autoclaved; the latter two stock solutions were filter-sterilized and added to room-temperature, sterile nutrient solution. Magenta boxes were filled in the sterile hood at the time of sowing. The low-strength nutrient solution described in ref. 6 was used for root exudation experiments.

For root growth experiments, surface-sterilized and stratified seeds were sown in 0.1% (wt/vol) agar in single files parallel to the outer edge of the magenta box. Six and 8 d from sowing, plants were photographed with a Kodak DCS760 digital camera with a Nikon AF Micro Nikkor 60-mm lens set to f4 (Photographic, Richmond, VA). Once focused on the first set of plants in a

given experiment, the camera was left in this position, focused on that particular shallow focal plane. Subjects were manually focused as necessary; a 1-cm scale ruler was also photographed. Images were transferred to an Apple PowerBook G4 by using Kodak DCS PHOTO DESK 4.3 for Macintosh, cropped, brightness/contrast-adjusted by using PHOTOSHOP 7 (Adobe Systems, San Jose, CA) for Macintosh, and then saved as TIFF files. The TIFF files were opened with IMAGEJ 1.34R for Macintosh for root measurements. Root measurements were collated in EXCEL X for Macintosh (Microsoft), and statistical analyses were performed by using MINITAB 14.2 (Minitab, State College, PA) for WINDOWS.

For RNA isolation and root exudate profiling, ≈500 seeds were planted on polypropylene mesh and grown for 6 d by using the high-strength medium without Al. For RNA isolation and Northern blot analysis, nutrient solutions were exchanged for the same solution with or without Al. Roots were collected in liquid N₂, and total RNA was isolated by using TRIzol reagent (Invitrogen) according to the manufacturer's instructions with minor modifications. Total RNA (10 μg per sample) was separated by electrophoresis on a Mops/formaldehyde agarose gel, transferred to Hybond N⁺ membranes (Amersham Pharmacia) according to the manufacturer's recommendations, and fixed at 80°C for 2 h. For the Northern blot analysis, a 376-bp fragment spanning the 3' end of the coding region (63 bp) and the 3' UTR (remaining 313 bp) of *AtALMT1* was used as a probe (see Table 3, which is published as supporting information on the PNAS web site). This probe shares only 36 bp of identity with *AtALMT2*. Purified PCR fragments were labeled with [³²P]dCTP by random priming, and membranes were hybridized and washed according to Sambrook *et al.* (22).

For root exudate profiling, nutrient solutions were exchanged for low ionic strength solution with or without Al as described in ref. 6. For the genetic complementation experiment, root exudate profiling was performed on groups of 10–20 plants. After photographing the plants at 6 d from sowing, the polypropylene mesh was cut into 1-cm squares under sterile conditions and transferred to flat-bottomed, six-well culture plates (Fisher Scientific) with 2 ml of low-strength nutrient solution. Analysis of root exudates for organic acid and inorganic anions was conducted by capillary electrophoresis (10).

Linkage Analysis, Gene Cloning, and Sequencing. Genetic linkage analysis was conducted by using standard PCR methodologies. Twenty-two genetic markers were designed by using polymorphism information from the Monsanto database (Table 3) (23).

AtALMT1 was cloned from six ecotypes: Col, Ler, Niederzenz, Nossen, Bayreuth, and Cape Verde Islands (GenBank accession nos. DQ465038–DQ465042). Compared with the Col reference sequence, this 3,074-bp amplicon contained 530 bp 5' to the translational start, the coding region (2,230 bp), and 314 bp of the 3' UTR. Amplified fragments were gel-purified and T₄-cloned into TOPO-XL (Invitrogen) before sequencing (see Table 2 for primer sequences). Nucleotide polymorphism among alleles was estimated by using Θ , where $\Theta = S_n / (a_{n-1})(n)$, S_n is the number of polymorphic sites, n is the length of sequence, and $a_{n-1} = \sum 1/i$ from 1 to $n - 1$, where i is the number of sequences compared (17).

Statistical Analyses. ANOVA were used to test whether experimental treatments or genotypic differences were correlated with significant differences. For the QTL mapping analysis, a correlation analysis was used to test the relationship between genotype and phenotype. Median root growth for each F₃ family was correlated with the allele state of its F₂ progenitor at 22 markers across 3.6 megabases by calculating a correlation coefficient r . The r value was then squared, and its significance was considered against an empirically calculated threshold by using bootstrapped data ($n = 1,000$; $r^2 > 0.10$ for $\alpha = 0.05$). Similar results

were obtained by using ANOVA, suggesting that the bootstrapped correlation analysis was statistically rigorous.

Electrophysiological Methodologies: *In Vitro* Transcription, Oocyte Injection, and Electrophysiological Recordings. cRNA was prepared by using the RNA Capping kit (Stratagene) according to the manufacturer's instructions with ScaI-digested pGEM-4Z plasmid DNA, which contained the *AtALMT1* coding region cloned from ecotype Col between the 3' and 5' UTRs of a *Xenopus* β -globin gene. Harvesting of stage V–VI *X. laevis* oocytes was performed as described by Golding (24). Defolliculated oocytes were maintained in ND96 solution (supplemented with 50 μ g/ml gentamycin) overnight before injections. *X. laevis* oocytes were injected with 48 nl of water containing 30 ng of cRNA encoding *AtALMT1* (or 48 nl of water as control) and incubated in ND96 at 18°C for 2–4 d. Whole-cell currents from oocytes expressing *AtALMT1* were recorded under constant perfusion at room temperature (22°C) with a GeneClamp 500 amplifier (Axon Instruments, Union City, CA) by using conventional two-electrode voltage-clamp techniques. Recording electrodes filled with 0.5 M K_2SO_4 and 30 mM KCl had resistances between 0.5 and 1.2 megaohms. Recordings were performed in oocytes that were or were not preloaded with malate by injecting 50 nl of 0.1 M sodium malate or water 2 h before electrophysiological

recordings. Recordings were performed in a solution consisting of 96 mM Mes, 1.8 mM $CaCl_2$, 2 mM KCl, and 0.1 mM $LaCl_3$, with or without 0.1 $AlCl_3$ and with the pH adjusted to 4.5. The ionic composition of this solution was chosen to attenuate the major voltage-dependent, hyperpolarization-induced, and volume-sensitive endogenous oocyte chloride currents (25). Liquid junction potentials were corrected as described by Neher (26). The holding potential was set to 0 mV, and voltage test pulses (400 ms in duration) were stepped between +10 mV and –200 mV (in 10-mV increments) with a 10-s resting phase at 0 mV between each voltage pulse. The current–voltage (*I/V*) relationships measured under different conditions were constructed by measuring the current amplitude at the end of the test pulses.

We thank K. Dunham, V. Hodgkinson, E. Craft, A. Clark, and T. DiMenna for technical assistance; the greenhouse staff of the Boyce Thompson Institute for Plant Research; and the *Arabidopsis* Biological Resource Center, the SIGNAL collection of the Salk Institute for Biological Studies, and G. Rairdan (Boyce Thompson Institute for Plant Research) for seed stocks. This work was supported by U.S. Department of Agriculture National Research Initiative Grant 02-35100-12058 (to O.A.H. and L.V.K.), U.S. Department of Agriculture–Agricultural Research Service Base Funds (to L.V.K.), and predoctoral fellowships from Coordenação de Aperfeiçoamento de Pessoal de Nível Superior (Brazil) (to L.G.M. and G.M.A.C.).

1. Wood, S., Sebastian, K. & Scherr, S. (2000) in *Pilot Analysis of Global Ecosystems: Agroecosystems* (Int. Food Policy Res. Inst. and World Resources Inst., Washington, DC), pp. 45–54.
2. Kochian, L. V. (1995) *Annu. Rev. Plant Physiol. Plant Mol. Biol.* **46**, 237–260.
3. Jackson, T. & Reisenauer, H. (1984) in *Soil Acidity and Liming*, ed. Adams, F. (Am. Soc. Agronomy, Crop Sci. Soc. Am., and Soil Sci. Soc. Am., Madison, WI), pp. 333–347.
4. Rao, I. M., Zeigler, R. S., Vera, R. & Sarkarung, S. (1993) *Bioscience* **43**, 454–465.
5. Kochian, L. V., Hoekenga, O. A. & Pineros, M. A. (2004) *Annu. Rev. Plant Physiol. Plant Mol. Biol.* **55**, 459–493.
6. Hoekenga, O. A., Vision, T. J., Shaff, J. E., Monforte, A. J., Lee, G. P., Howell, S. H. & Kochian, L. V. (2003) *Plant Physiol.* **132**, 936–948.
7. Ryan, P. R., Delhaize, E. & Randall, P. J. (1995) *Planta* **196**, 103–110.
8. Pellet, D., Grunes, D. & Kochian, L. (1995) *Planta* **196**, 788–795.
9. Ryan, P. R., Delhaize, E. & Randall, P. J. (1995) *Aust. J. Plant Physiol.* **22**, 531–536.
10. Pineros, M. A., Shaff, J. E., Manslank, H. S., Alves, V. M. & Kochian, L. V. (2005) *Plant Physiol.* **137**, 231–241.
11. Sasaki, T., Yamamoto, Y., Ezaki, B., Katsuhara, M., Ahn, S. J., Ryan, P. R., Delhaize, E. & Matsumoto, H. (2004) *Plant J.* **37**, 645–653.
12. Raman, H., Zhang, K., Cakir, Z., Appels, R., Garvin, D. F., Maron, L. G., Kochian, L., Moroni, J. S., Raman, R., Imtiaz, M., et al. (2005) *Genome* **48**, 781–791.
13. Yamaguchi, M., Sasaki, T., Sivaguru, M., Yamamoto, Y., Osawa, H., Ahn, S. J. & Matsumoto, H. (2005) *Plant Cell Physiol.* **46**, 812–816.
14. Meyers, B. C., Kozik, A., Griego, A., Kuang, H. & Michelmore, R. W. (2003) *Plant Cell* **15**, 809–834.
15. Birnbaum, K., Shasha, D. E., Wang, J. Y., Jung, J. W., Lambert, G. M., Galbraith, D. W. & Benfey, P. N. (2003) *Science* **302**, 1956–1960.
16. Alonso, J. M., Stepanova, A. N., Leisse, T. J., Kim, C. J., Chen, H., Shinn, P., Stevenson, D. K., Zimmerman, J., Barajas, P., Cheuk, R., et al. (2003) *Science* **301**, 653–657.
17. Watterson, G. A. (1975) *Theor. Popul. Biol.* **7**, 256–276.
18. Schmid, K. J., Ramos-Onsins, S., Ringys-Beckstein, H., Weisshaar, B. & Mitchell-Olds, T. (2005) *Genetics* **169**, 1601–1615.
19. Kobayashi, Y. & Koyama, H. (2002) *Plant Cell Physiol.* **43**, 1526–1533.
20. Lister, C. & Dean, C. (1993) *Plant J.* **4**, 745–750.
21. Delhaize, E., Ryan, P. R., Hebb, D. M., Yamamoto, Y., Sasaki, T. & Matsumoto, H. (2004) *Proc. Natl. Acad. Sci. USA* **101**, 15249–15254.
22. Sambrook, J., Fritsch, E. F. & Maniatis, T. (1989) in *Molecular Cloning: A Laboratory Manual*, eds. Ford, N., Nolan, C. & Ferguson, M. (Cold Spring Harbor Lab. Press, Plainview, NY), pp. 7.37–7.52.
23. Jander, G., Norris, S. R., Rounsley, S. D., Bush, D. F., Levin, I. M. & Last, R. L. (2002) *Plant Physiol.* **129**, 440–450.
24. Golding, A. L. (1992) in *Methods in Enzymology*, eds. Rudy, B. & Iverson, L. E. (Academic, London), Vol. 207, pp. 266–279.
25. Mitcheson, J. S., Chen, J. & Sanguinetti, M. C. (2000) *J. Gen. Physiol.* **115**, 229–240.
26. Neher, E. (1992) *Methods Enzymol.* **207**, 123–131.